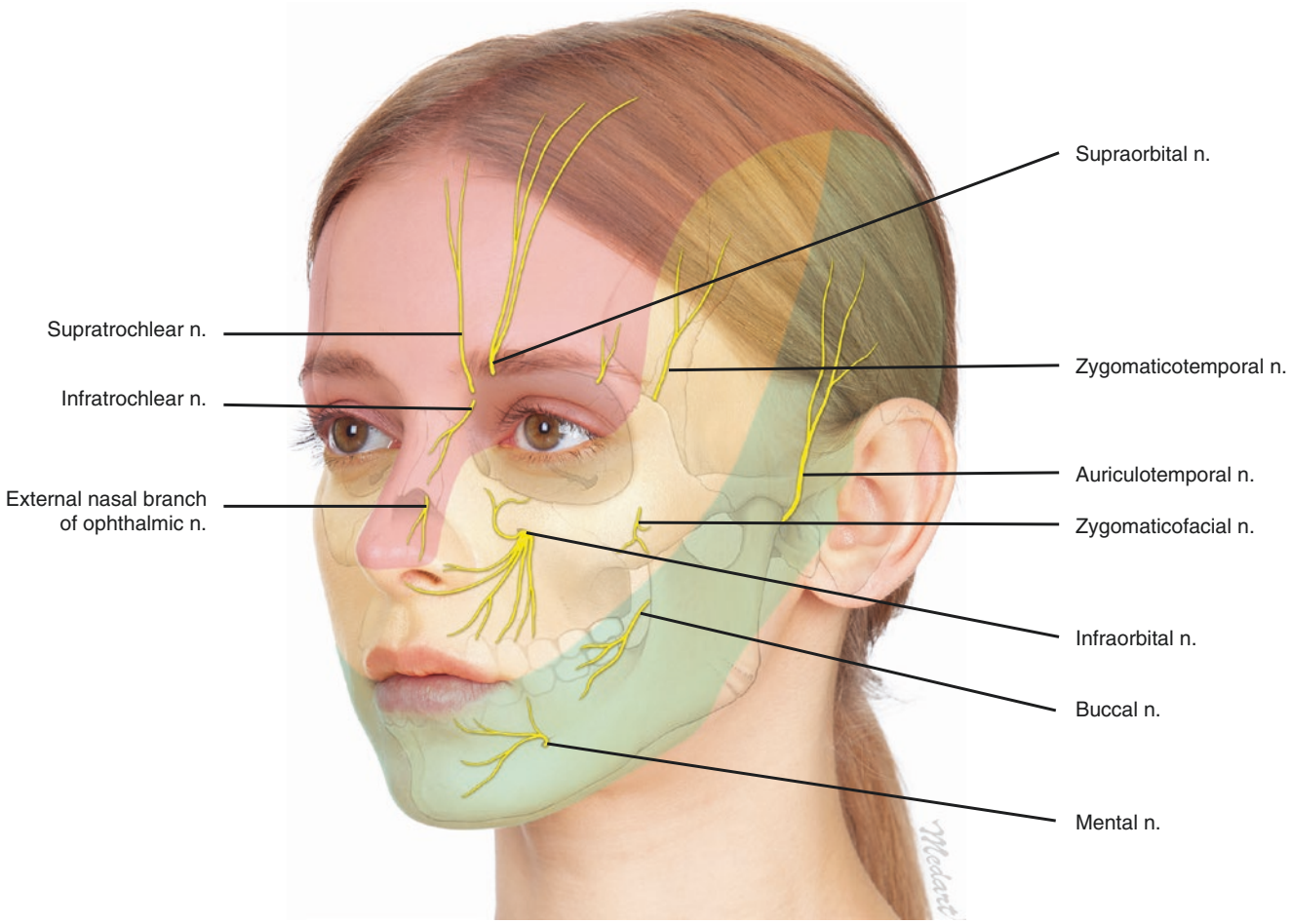

Fig. 2.10 The cutaneous sensory distribution of the face (red zone area of the ophthalmic nerve (V1) branches, yellow zone area of the maxillary nerve (V2) branches, green zone area of the mandibular nerve (V3) branches). (Published with kind permission of © Kwan-Hyun Youn 2020. All Rights Reserved)

matic, buccal, marginal mandibular, and cervical nerve branches. These minute nerve branches are randomly dispersed into muscles making it difficult to determine the nerve innervation of specific muscle (Fig. 2.11b).

2.2 US Images of the Normal Facial Skin, Subcutaneous Tissues, and Gland

It is well known that the thinnest part of the facial skin is located at the upper eyelid (0.38–0.80 mm) and the thickest at the nose ala, nose tip, and chin (1.22–2.01 mm). Recent studies demonstrated that the skin layer at the anterior cheek and mental region is relatively thicker. The facial skin was more than 2.0 mm thick at landmarks on the pogonion, zygion, and cheek. This concludes that the facial skin is thicker in the chin, lower face, and zygomatic arch area than the other areas (Table 2.1; Figs. 2.12 and 2.13).

On the US images, the epidermis and dermis can be observed from the facial and cervical skin. The epidermis is the outer layer of the skin, and dermis is right beneath the epidermis. The skin has echogenic properties due to the keratinized layer; however, the dermis is relatively less hyperechoic compared to the epidermis for its high collagen content. The echogenicity of the dermis varies due to the regional differences in the thickness of the dermis (Figs. 2.14 and 2.15).

The spatial relationship of the soft tissues of the face can be classified by layers. Deep to the skin is the subcutaneous fat tissue with superficial and deep layers. The superficial layer of subcutaneous fat tissue covers the whole face. The deep layer of subcutaneous fat is located deep to the facial muscles and is demarcated by dense connective tissues such as the capsules or retaining ligaments. The characteristics of the deep layer of subcutaneous fat are different from the superficial layer. The suborbicularis oculi fat (SOOF), retro-

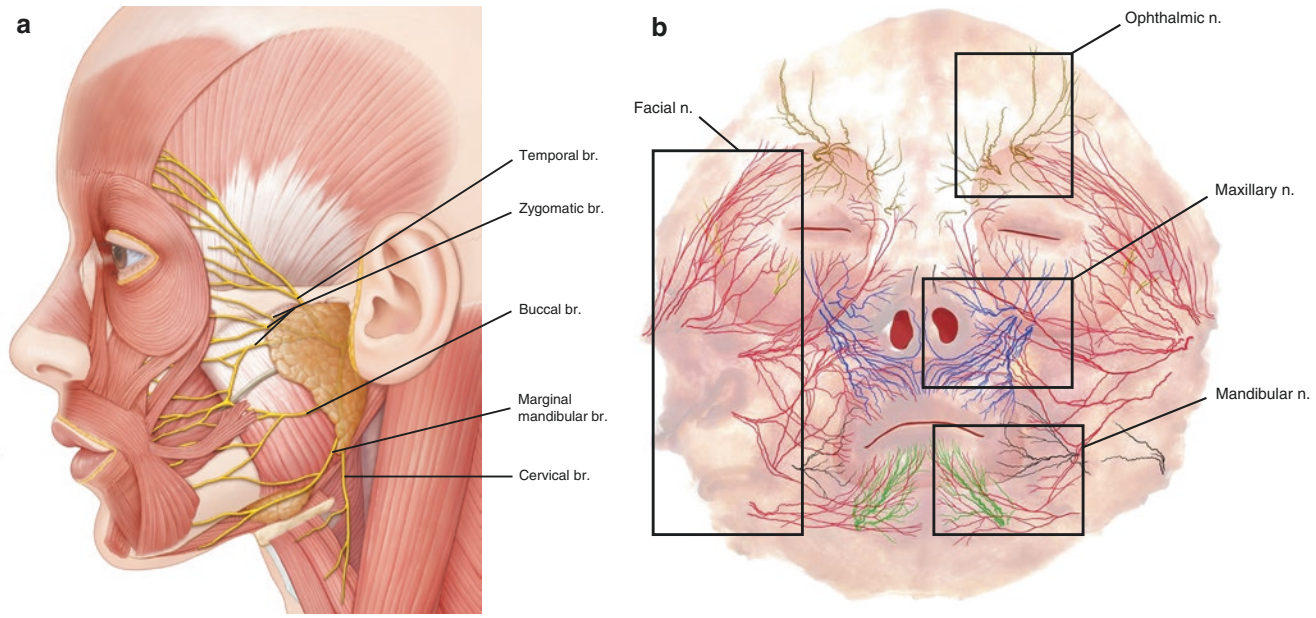

Fig. 2.11 Topography of the facial nerve. (**a**) Facial nerve and its temporofacial and cervicofacial divisions and (**b**) sensory and motor nerve distribution on the face. (Published with kind permission of © Hee-Jin Kim and Kwan-Hyun Youn 2020. All Rights Reserved)

Table 2.1 Overall thicknesses of the facial skin and superficial fat based on the anatomical regions

	Skin		Superficial fat	
Regions	Mean	SD	Mean	SD
Forehead	1.70	0.71	1.99	1.21
Radix and dorsum	1.51	0.55	1.61	1.07
Supraorbital	1.67	0.83	1.82	1.22
Infraorbital	1.97	0.84	4.93	2.98
Perioral	1.82	0.83	5.14	3.31
Temple	1.65	0.91	2.58	1.68
Cheek	1.85	1.03	4.54	2.71

Unit: mm
SD standard deviation

orbicularis oculi fat (ROOF), buccal fat, and deep cheek fat are considered deep fat layers of the face. Fibrous connective tissues pass through facial fat tissues and contribute to connecting the fat tissue, facial muscles, dermis, and bone (Fig. 2.16).

The superficial fascia, or subcutaneous connective tissue, contains unequal amounts of fat tissue, which are broadly distributed between facial musculature and the skin. The buccal fat is an encapsulated pad that forms bulged cheeks that are connected to the scalp and temple region. The facial v., the trigeminal n., the facial n., and the superficial facial m. lie within the subcutaneous tissue (Fig. 2.17).

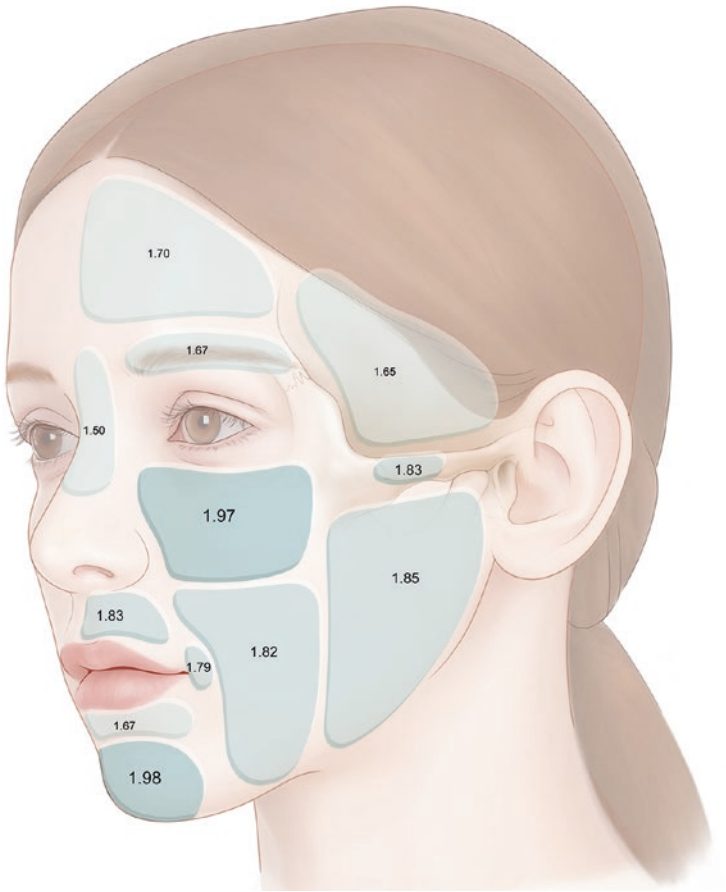

Fig. 2.12 Mean skin thickness of the face based on anatomical regions. (Published with kind permission of © Kwan-Hyun Youn 2020. All Rights Reserved)

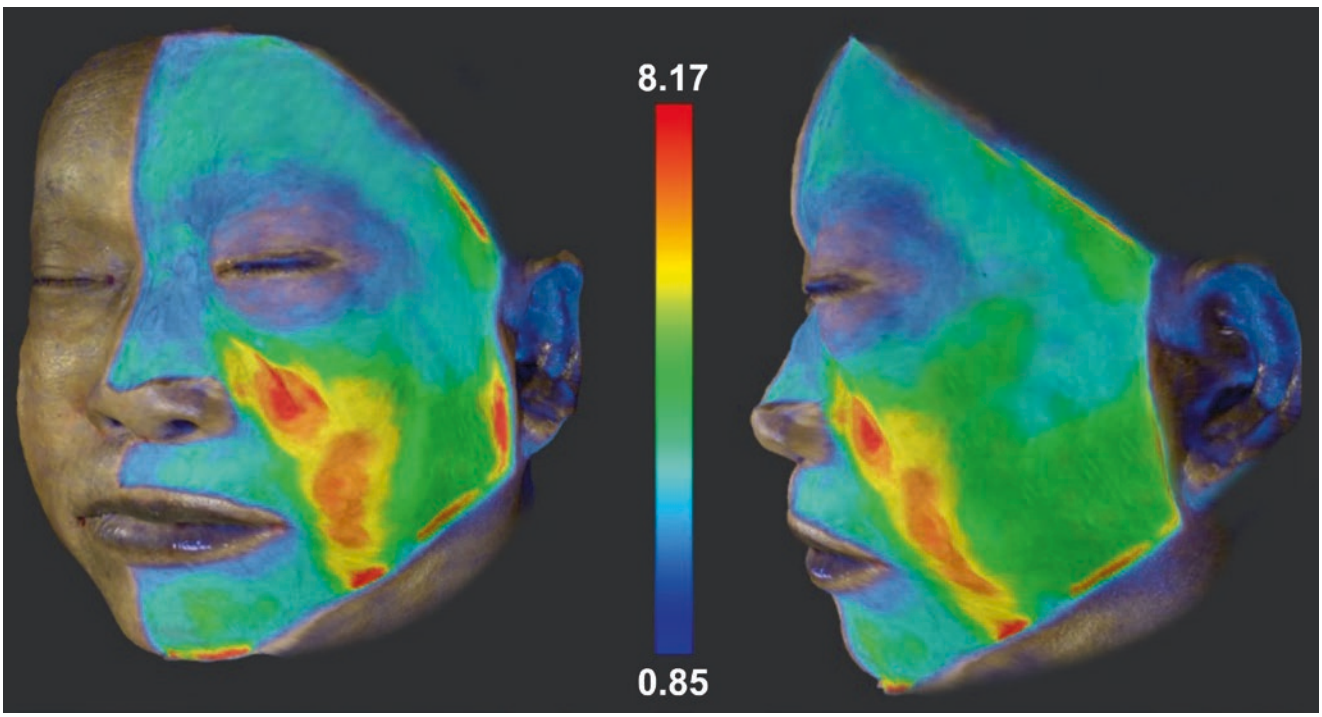

Fig. 2.13 3D images representing the mean thickness of the subcutaneous layer of the face (unit: mm). (Published with kind permission of © Hee-Jin Kim 2020. All Rights Reserved)

The subcutaneous tissue (called subcutis or hypodermis) is shown as a hypoechoic layer because of its fatty lobules. Between the fatty lobules, hyperechoic linear fibrous septa can be seen. The level of hypoechogenicity varies depending on the fat component (dense or loose) (Fig. 2.18).

There are three major salivary glands in the facial area: parotid, submandibular, and sublingual glands. There are also several minor salivary glands located in the submucosal region of the lips and so on. The parotid gland is the largest major salivary gland and situated on the posterior border of the mandible and above and below the mandibular angle. It is divided into superficial and deep layers. The superficial layer is located on the masseteric fascia, and the deep layer overlays the masseter m. and the mandible and covers the medial side of the mandibular ramus (Fig. 2.19).

There are frequent anatomical variants in the prominence of the parotid gland in the superficial upper 1/3 of the masseter m. Another anatomical variant is the accessory parotid gland, which is located superficial to the masseter m. but separated from the main parotid gland (Fig. 2.20).

The submandibular gland is located within the submandibular triangle of the neck. It lies inferior to the mandible and superficial to the mylohyoid m. It is the second largest major salivary gland, and its size is similar to that of a walnut. The submandibular gland is divided into the superficial and deep portions relative to the posterior free margin of the mylohyoid m. (Figs. 2.19 and 2.21).

Minor salivary glands are located beneath the oral mucosa and are distributed all over the face, lips, tongue, tonsil, buccal cheek, and palate (Fig. 2.22). The parotid and submandibular glands are hyperechoic in comparison with the adjacent muscles (Figs. 2.19 and 2.21), while the minor salivary glands are hypoechoic. The submucosal minor salivary glands located in the oral mucosa appear as well-defined, round, hypoechoic structures (Fig. 2.23).

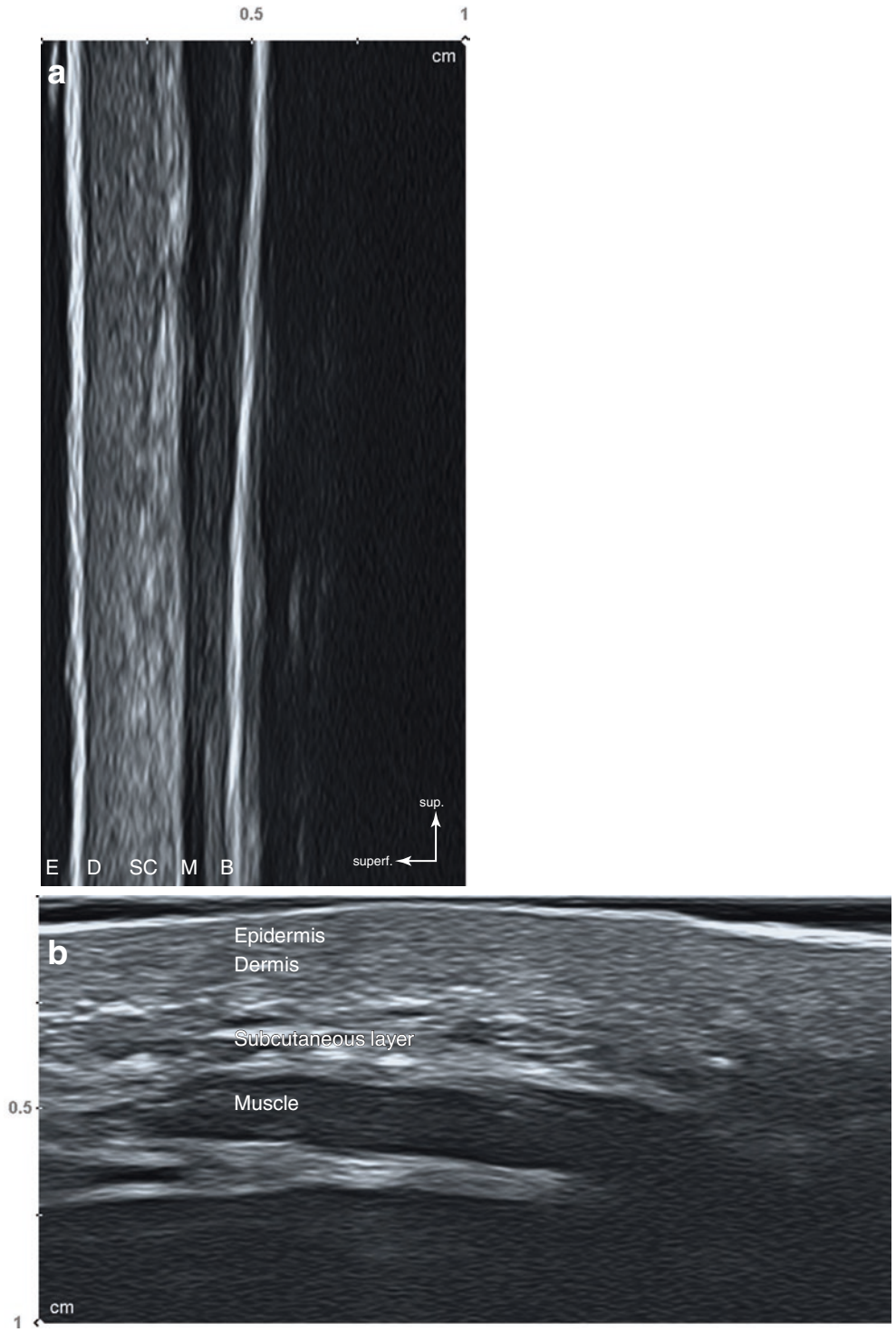

Fig. 2.14 Ultrasonography representing the regional difference of the epidermis (E), dermis (D), subcutaneous tissue (SC), muscle (M), and bone (B). (**a**) Radix (sagittal view, 24 MHz by linear transducer) and (**b**) subzygomatic area (transverse view, 24 MHz by linear transducer). (Published with kind permission of © Hee-Jin Kim 2020. All Rights Reserved)

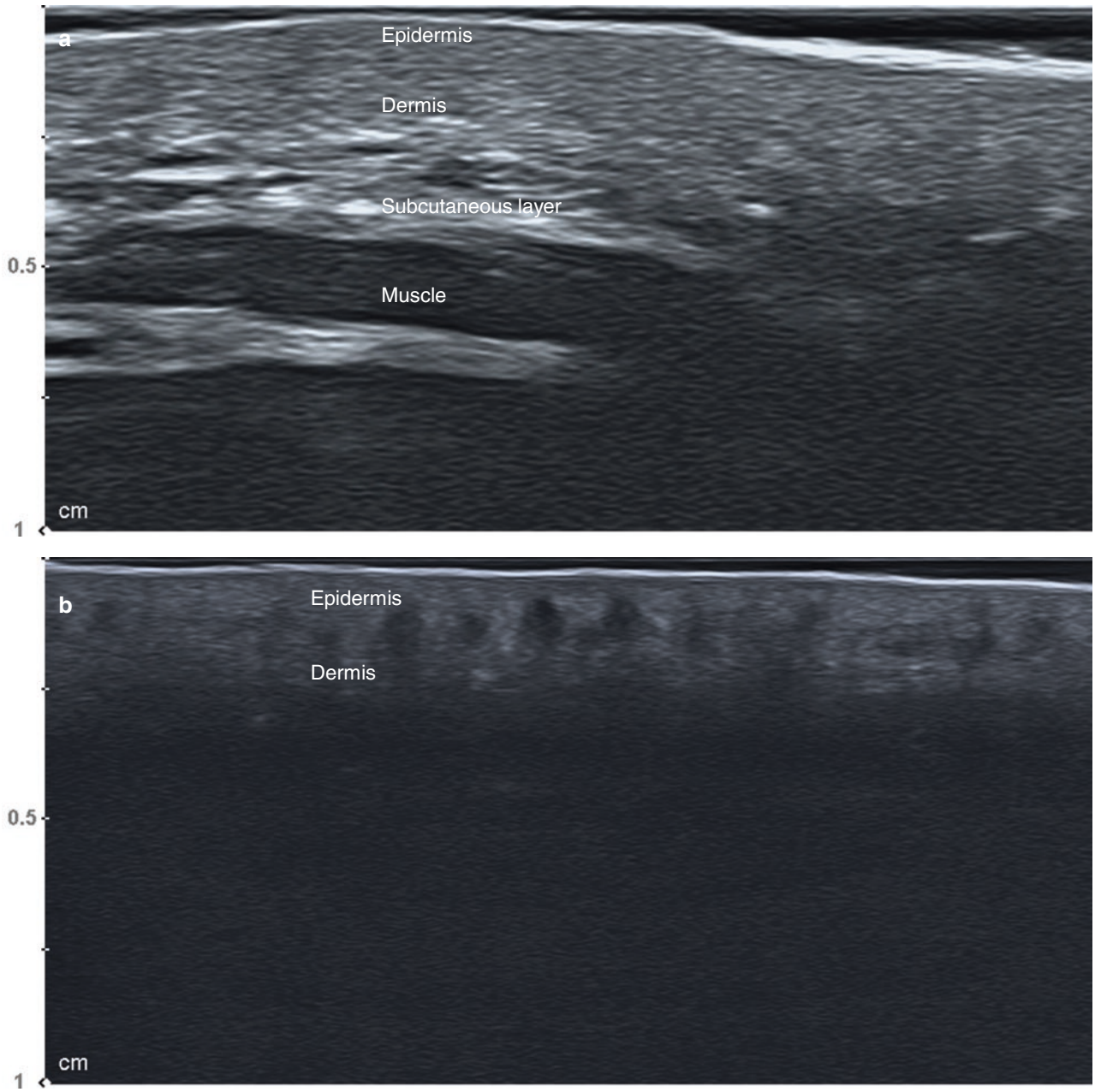

Fig. 2.15 Differences in image resolution of the ultrasonography depending on the frequency. (**a**) 24 MHz by linear transducer (subzygomatic area, transverse view) and (**b**) 32 MHz by linear transducer (subzygomatic area, transverse view). (Published with kind permission of © Hee-Jin Kim 2020. All Rights Reserved)

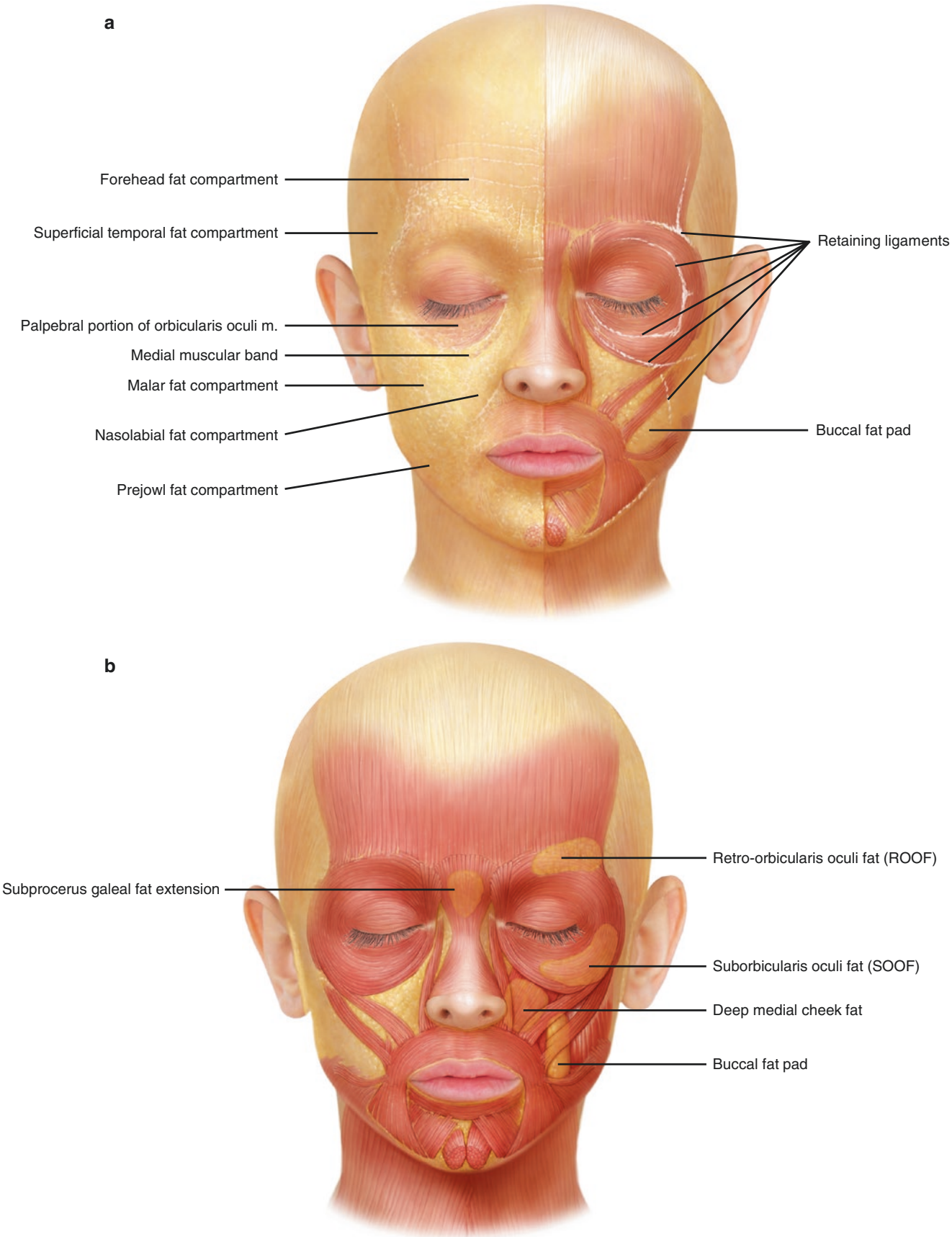

Fig. 2.16 Facial fat compartments. (**a**) Subcutaneous fat and superficial muscles of the face and (**b**) deep fat compartments of the face. (Published with kind permission of © Kwan-Hyun Youn 2020. All Rights Reserved)

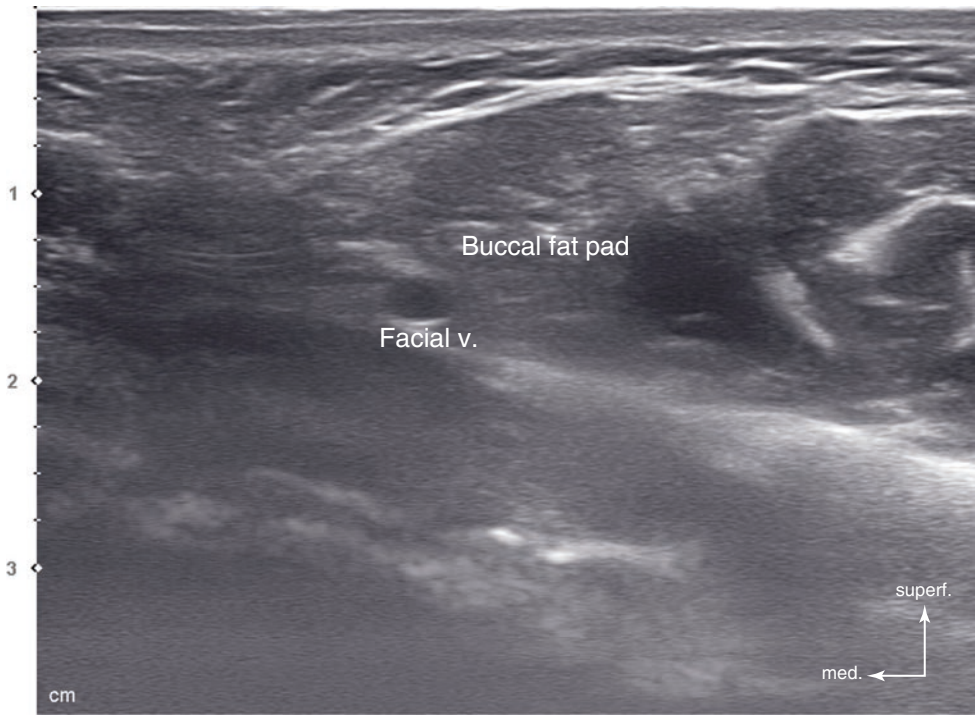

Fig. 2.17 Ultrasonography representing buccal fat pad (transverse view, 15 MHz by linear transducer). (Published with kind permission of © Hee-Jin Kim 2020. All Rights Reserved)

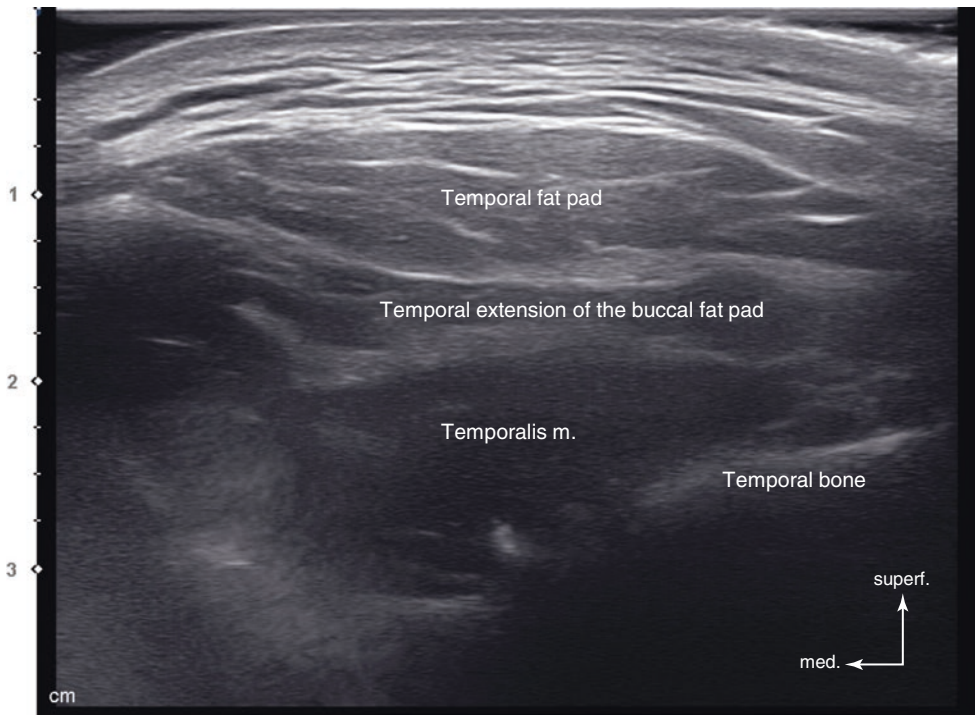

Fig. 2.18 Variable hypoechogenecity depending on the fat compartments of the temple. (Published with kind permission of © Hee-Jin Kim 2020. All Rights Reserved)

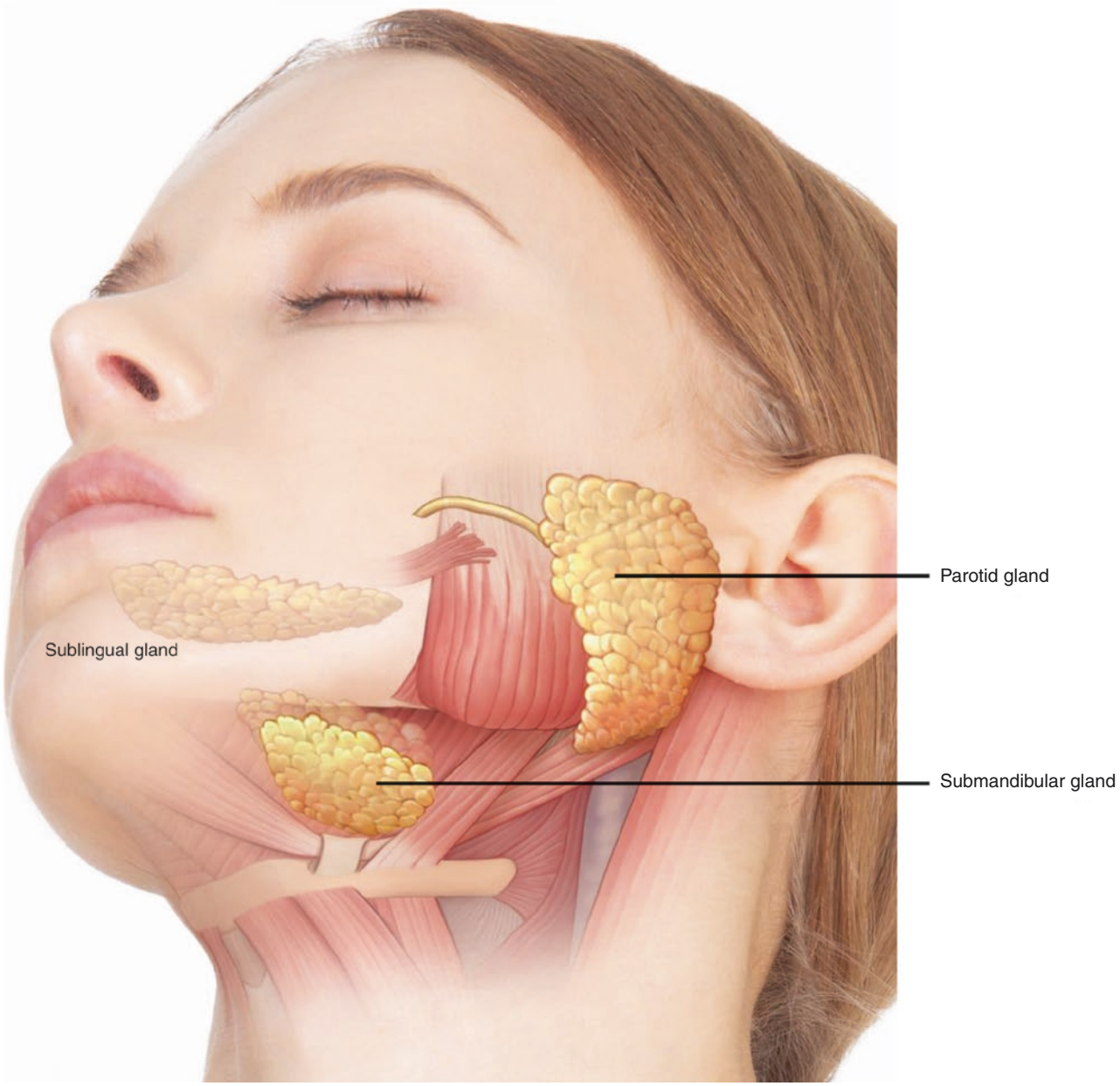

Fig. 2.19 Illustration of three major salivary glands. (Published with kind permission of © Kwan-Hyun Youn 2020. All Rights Reserved)

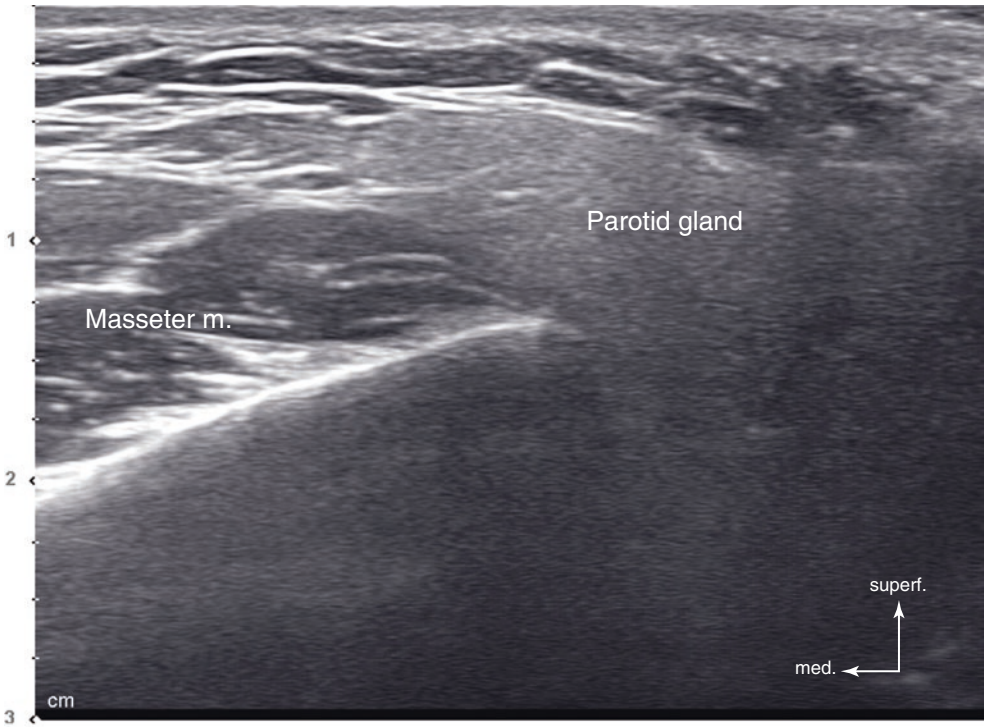

Fig. 2.20 Ultrasonography of the parotid gland (transverse view, 15 MHz by linear transducer). (Published with kind permission of © Hee-Jin Kim 2020. All Rights Reserved)

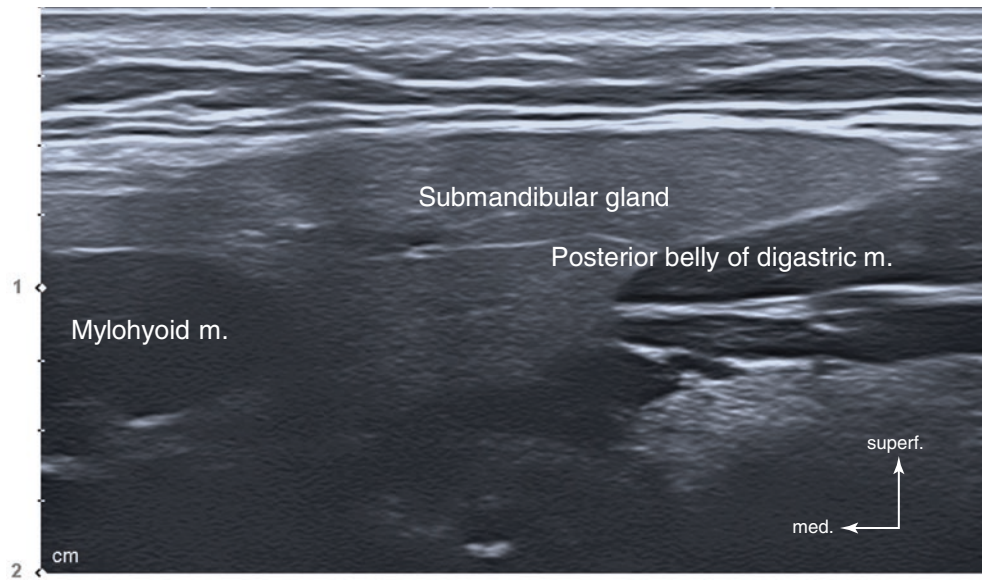

Fig. 2.21 Ultrasonography of the submandibular gland (transverse view, 15 MHz by linear transducer). (Published with kind permission of © Hee-Jin Kim 2020. All Rights Reserved)

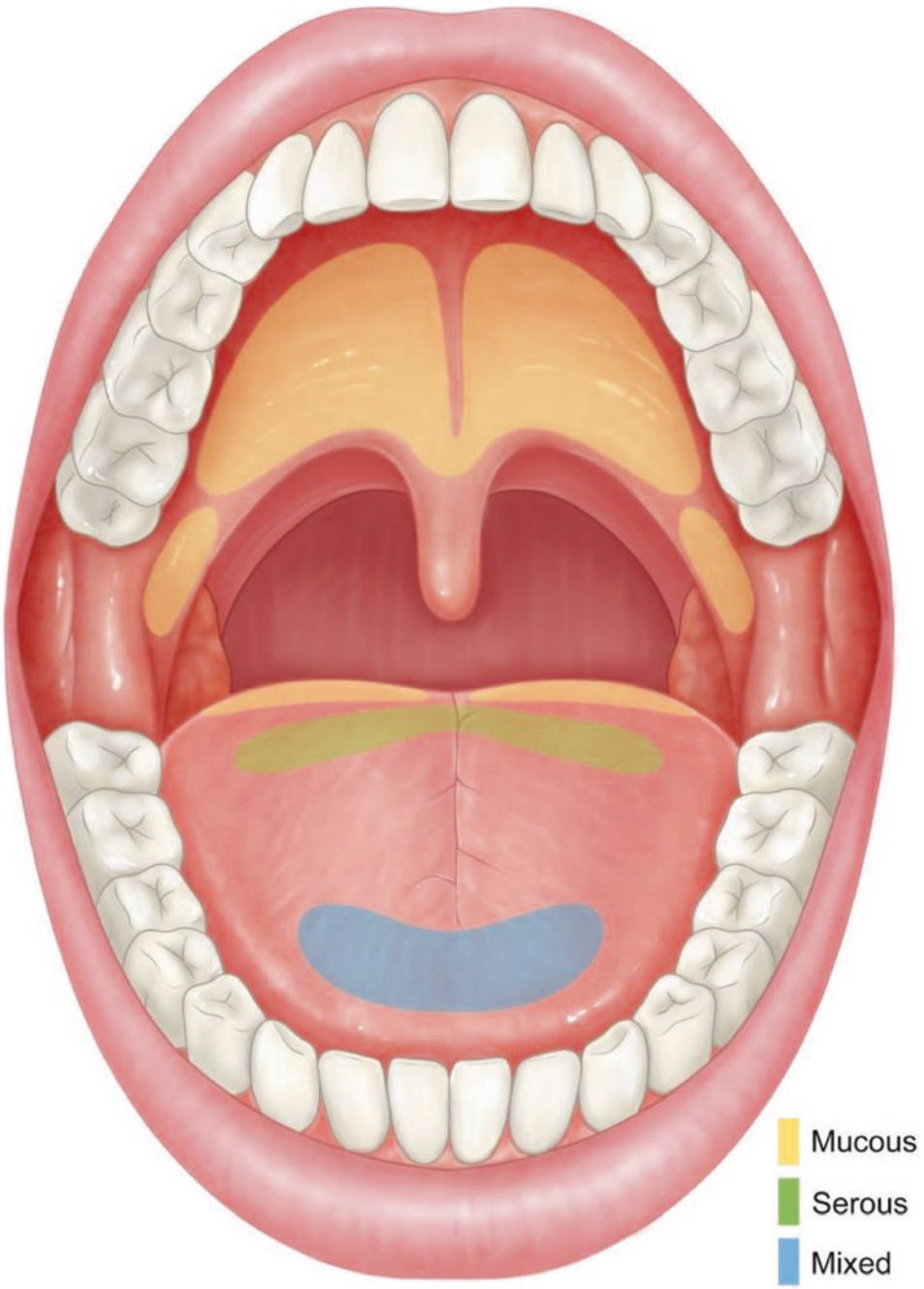

Fig. 2.22 Illustration of the locations and components of the minor salivary glands. (Published with kind permission of © Kwan-Hyun Youn 2020. All Rights Reserved)

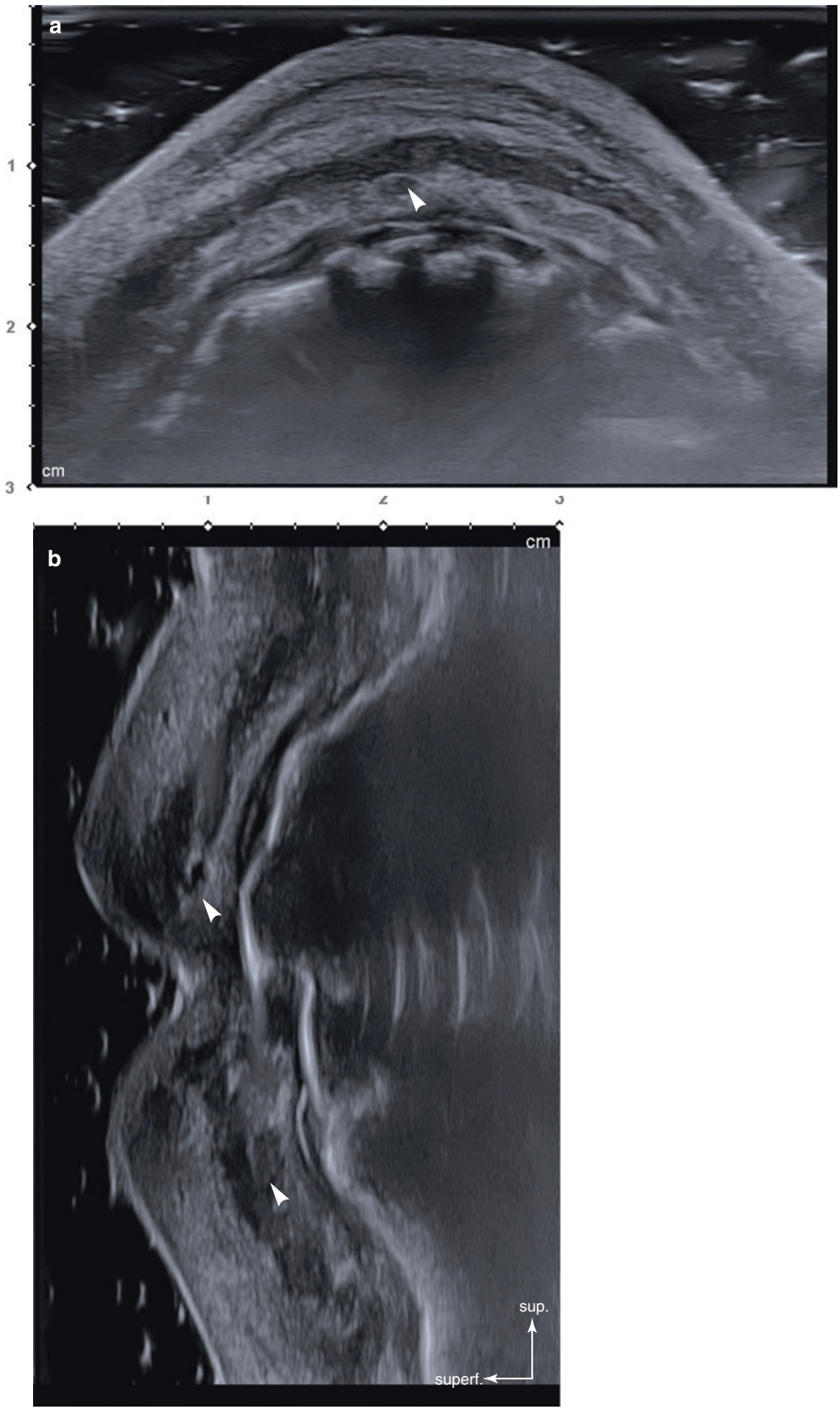

Fig. 2.23 Ultrasonography representing the minor salivary glands (arrowheads) of the lip. (**a**) Transverse view, 15 MHz by linear transducer and (**b**) sagittal view, 15 MHz by linear transducer. (Published with kind permission of © Hee-Jin Kim 2020. All Rights Reserved)